Anion Adsorption, CO Oxidation, and Oxygen Reduction Reaction on a Au(100) Surface: The pH Effect

B. B. Blizanac, C. A Lucas,† M. E. Gallagher,† M. Arenz, P. N. Ross, and N. M. Marković*

Materials Sciences Division Lawrence Berkeley National Laboratory, University of California, Berkeley, California 94720

Received: August 21, 2003; In Final Form: October 29, 2003

The effects of pH on the surface reconstruction of Au(100), on CO oxidation, and on the oxygen reduction reaction (ORR) have been studied by a combination of surface X-ray scattering (SXS), Fourier transform infrared (FTIR) spectroscopy, and rotating ring-disk electrode (RRDE) measurements. In harmony with previous SXS and scanning tunneling microscopy (STM) results, the potential-induced hexagonal ("hex") to (1 × 1) transition occurs faster in an alkaline electrolyte than in acidic media. In alkaline solution, CO adsorption facilitates the formation of a "hex" phase; in acid solution, however, CO has negligible effect on the potential range of thermodynamic stability of the "hex" ↔ (1 × 1) transition. We propose that in KOH the continuous removal of OH_{ad} in the Langmuir−Hinshelwood reaction ($CO + OH = CO_2 + H^+ + e^-$) may stabilize the "hex" phase over a much wider potential range than in CO-free solution. In acid solution, where specifically adsorbing anions cannot be displaced by CO from the Au(100) surface, CO has negligible effect on the equilibrium potential for the "hex" ↔ (1 × 1) transition. Such a mechanism is in agreement with the pH-dependent oxidation of CO. The ORR is also affected by the pH of solution. It is proposed that the pH-dependent kinetics of the ORR on Au(100) can be unraveled by finding the relationship between kinetic rates and two terms: (i) the energetic term of the Au(100)−O_2^- interaction determines the potential regions where the rate-determining step $O_2 + e = O_2^-$ occurs, and (ii) the preexponential term determines the availability of active sites for the adsorption of O_2^-.

1. Introduction

The correlation between surface structure and reactivity is of central importance in surface electrochemistry. In the past decade this correlation has been successfully explored via combined electrochemical and surface-science studies on single crystals with different exposed planes. A prime example of the success is the recent study of fuel cell reactions on platinum single-crystal surfaces.[1] Just as for the surface processes at the Pt(*hkl*) electrodes, the electrochemical reactions at well-characterized Au(*hkl*) surfaces in an electrochemical environment are also dependent on the arrangement of surface atoms. In fact, a direct relationship between the kinetic rates of electrochemical reaction and the surface structure of metal electrodes has been found for the ORR on gold single-crystal surfaces.[2] In independent studies by two research groups,[3−5] the Au(100) surface in alkaline solution was found to be the most active of the low-index faces (by nearly 4 orders of magnitude) and was reported as even more active than polycrystalline platinum under the same experimental conditions. Despite efforts by many research groups to determine the origin of this catalytic activity,[3−7] the reason for this structure sensitivity remains unclear. Adzic and Marković reported that the unique catalytic activity of the Au(100) surface appears only in the potential region in which OH_{ad} is adsorbed on the surface.[3,4] On the basis of this evidence it was proposed that the change in the catalytic activity of the Au(100) surface from $4e^-$ to $2e^-$ reduction was possibly due to the existence of a AuOH layer. On the other hand, Peck and McIntire argued that the higher activity of Au(100) for the ORR was related to the dissociative adsorption of HO_2^- anions on the 4-fold symmetry sites that occur only on the (100)−(1 × 1) surface.[5] Consequently, it was proposed that the change in the oxygen reduction pathway from $4e^-$ to $2e^-$ reduction might be due to the potential-induced reconstruction of the (1 × 1) surface to a structure similar to the "hex" reconstruction found in UHV. The SXS-EC results in reference [8] unambiguously showed that the (1 × 1) ↔ "hex" reconstruction is not the dominant mechanism for this change in reaction pathway since the transition in reduction kinetics occurs over a narrower potential range than the (1 × 1) ↔ "hex" transition. Furthermore, the time constant for the two transitions differs by approximately 2 orders of magnitude, with the structural transition being the slower. Another related issue is the observed sensitivity of the "hex" ↔ (1 × 1) conversion to the nature of the electrolyte anions and the adsorption of carbon monoxide.[9] For example, using STM it has been shown that specific anion adsorption and the adsorption of CO shift the onset potential for the "hex" ↔ (1 × 1) transition and can enhance considerably the conversion dynamics. However, while in acid solution anion adsorption shifts the "equilibrium potential" of the "hex" ↔ (1 × 1) transition to lower values, the adsorption of CO in alkaline solution shifts the transition to more positive potentials.[9]

In this paper, we present a combined in-situ SXS/electrochemistry study of the Au(100) reconstruction in 0.1 M KOH, 0.1 M $HClO_4$ and 0.1 M $HClO_4$ containing Cl^- ions. We also report the results for the effects of adsorbed CO on triggering and controlling the formation of the "hex" ↔ (1 × 1) transition.

* Corresponding author. E-mail: nmmarkovic@lbl.gov.
† Oliver Lodge Laboratory, Department of Physics, University of Liverpool, Liverpool, L69 7ZE, U.K.

10.1021/jp036483l CCC: $27.50
Published on Web 12/11/2003

Besides enabling a comparison to be made between the effect of CO on the reconstruction in alkaline versus acid solution, the findings also shed some light on the energetics of the interaction of OH, Cl, and CO with the Au(100) surface in these two electrolytes. As part of a detailed study of substrate−adlayer structure on Au(100) by SXS, we have also examined the interrelationship between the "hex" ↔ (1 × 1) transition and the ORR kinetics in acid and alkaline electrolytes. Some pertinent observations along these lines, specifically the pH effect in the catalysis of oxygen reduction and CO oxidation reactions on Au(100), are given in this paper.

2. Experimental Section

2.1. Electrochemical Measurements. The pretreatment and assembly of the Au(100) single crystal (0.283 cm^2) into a RRDE configuration was described previously,[10] e.g., the crystal was flame annealed in a propane flame and cooled in an Ar atmosphere before being mounted in the RRDE setup. Subsequently, the electrodes were transferred into a thermostated standard three-compartment electrochemical cell and immersed into the Ar-purged electrolyte at ≈298 K (Ar: *Bay Gas Research Purity*; 0.1 M $HClO_4$, 0.1 M KOH: *Aldrich Semiconductor Grade* prepared with triply pyrodistilled water) under potentiostatic control at ≈0.1 V. The reference electrode was a saturated calomel electrode (SCE) separated by a closed electrolyte bridge from the working electrode compartment in order to avoid chloride contamination. All potentials, however, refer to that of the reversible hydrogen electrode in the same electrolyte. The collection efficiency of the RRDE setup was N = 0.22 ± 5%.

2.2. SXS Measurements. The general experimental procedure used in X-ray diffraction measurements of electrochemical systems has been described in detail in previous articles.[11−13] As for electrochemical measurements, the crystal (miscut <0.1°) was transferred into the X-ray electrochemical cell. The cell was mounted at the center of a four-circle Huber goniometer on beamline 7-2 at the Stanford Synchrotron Radiation Laboratory (SSRL), using a 10 keV X-ray beam, defined by slits to be a 1 mm × 1 mm spot at the sample. Diffracted X-rays were measured by a Ge solid-state detector after passing through a Soller slit which defined an in-plane resolution of ca. 0.005 $Å^{-1}$. The crystal was indexed to the conventional bulk unit cell for the fcc(100) surface. Further experimental details can be found in the reference.[14]

2.3. FTIR Measurements. The in-situ FTIR measurements were taken with a Nicolet Nexus 670 spectrometer purged with nitrogen and equipped with a MCT detector cooled with liquid nitrogen. All IR measurements were performed in a spectroelectrochemical glass cell designed for an external reflection mode in a thin layer configuration. The cell is coupled at its bottom with a CaF_2 prism beveled at 60° from the surface normal. Prior to each measurement, a cyclic voltammogram was recorded in order to confirm the cleanliness of the electrode surface. Subsequently the solution was saturated with CO for at least 10 min, holding the electrode potential at −0.05 V. The spectra were recorded with a resolution of 8 cm^{-1}. All measurements were performed using p-polarized light. To obtain a single beam spectrum 50 scans were collected at each potential, resulting in a recording time of 25 s. Absorbance spectra were calculated as the ratio $-\log(R/R_0)$ where R and R_0 are the reflectance values corresponding to the sample and reference spectra, respectively. Reference spectra were recorded either at 1.5 V or −0.05 V, where CO_{ad} is completely oxidized and before the onset of CO_{ad} oxidation, respectively. The reference potential in the spectroelectrochemical cell was controlled by a RHE.

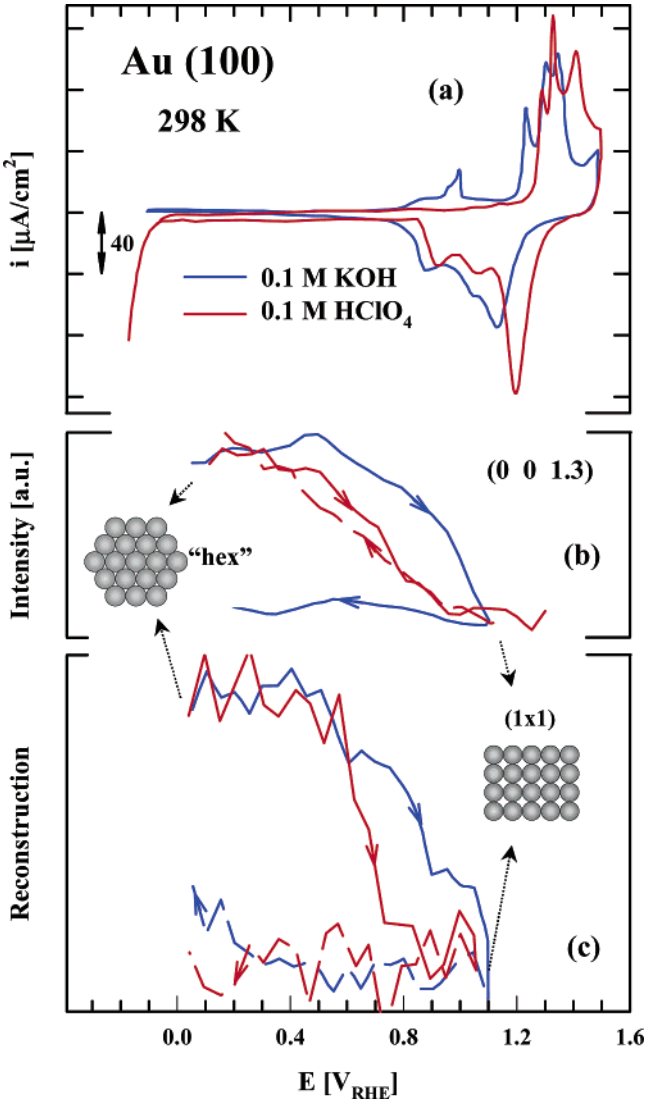

Figure 1. (a) The CV for a Au(100) electrode in 0.1 M $HClO_4$ and 0.1 M KOH at 298 K and 50 mV/s; (b) XRV measurements (2 mV/s) at (0, 0, 1.3), a position on the specular CTR; (c) XRV measurements (2.5 mV/s) close to reciprocal space position (1.2, 1.2, 0.4) at the rotated peak position in 0.1 M $HClO_4$ and unrotated peak position in 0.1 M KOH (see Figure 2). Ball models represent the "hex" and (1 × 1) surface structure.

3. Results and Discussion

3.1. Surface Characterization of Au(100) in $HClO_4$ and KOH. The ability to characterize atomic/molecular spatial structures and to monitor changes in the local symmetry of surface atoms in-situ under reaction conditions has played an important part in surface electrochemistry at monocrystalline metal electrodes. For example, SXS was used to demonstrate that Au(*hkl*) single-crystal surfaces in an electrochemical environment exhibit a potential-dependent reconstruction that is unique to the fcc metal surface.[11,15] The potential range of stability of the Au(100) reconstructed surfaces in both alkaline and acid electrolytes is shown in Figure 1 along with the base voltammograms. As shown in Figure 1a, there are two major differences between the cyclic voltammetry in alkaline solution with respect to acid media: (i) at lower potentials ($0.7 < E < 1.2$ V) the surface coverage by OH_{ad} is higher in alkaline than

in acid solution (ca. 60 μC/cm^2), and (ii) the onset of a "true" oxide formation is shifted negatively (by ca. 0.07 V) in the alkaline solution. This difference can be attributed to the competitive adsorption of OH_{ad} with anions from supporting electrolyte, i.e., in perchloric acid solution with ClO_4^- [16,17] and Cl^-.[18,19] Given that at $E < 0.7$ V the voltammetry shows the so-called "double layer" structure, the capacitance in this potential region should correspond exclusively to the charging/discharging of the interface. As we discuss in section 3.2, this explanation may not be correct, so that in addition to a pure capacitive component some faradaic (adsorption) processes may take place even in the "double layer" potential region. Furthermore, this adsorption will have an important role in the interpretation of potential-induced surface reconstruction, i.e., atomic surface arrangement that differs from the ideal bulk termination structure.

The potential stability of the Au(100) surface reconstruction in the electrochemical environment has been studied by cyclic voltammetry-ex-situ emersion LEED experiments,[20] STM,[20−22] and X-ray diffraction.[11,15] In both acid and alkaline solutions there is good agreement between the experimental techniques that the "5 × 20" reconstruction is formed at cathodic potentials and that it can be reversibly lifted and formed upon cycling the applied potential anodically. The (5 × 20) reconstruction gives rise to a hexagonal diffraction pattern in the surface plain of reciprocal space with the first-order reflections being close to the "anti-Bragg" positions. Figure 2 displays representative in-plane X-ray diffraction rocking scans (measured at 0.05 V) in 0.1 M KOH and 0.1 M $HClO_4$ solutions, respectively. In both cases the scattering due to the reconstructed surface is absent at higher potentials. In 0.1 M KOH, the scan shows either a single broad peak aligned with the [110] direction to (1.2, 1.2, 0.4), as reported previously[11] (Figure 2a), or two peaks rotated by 0.75° from the [110] direction (Figure 2b). At this point we have no explanation why in alkaline solution under very similar experimental conditions (i.e., flame annealing procedure, potential window of cycling, number of cycles, etc.) the reconstruction domains are different in two independent measurements. In 0.1 M $HClO_4$ (Figure 2c), however, the scan always displays two peaks which are rotated by ~0.75° from the [110] direction. Note that although there is also rotation in KOH the peaks are much broader, indicating that the structure in alkaline solution is more pinned to defects which may hinder the rotation. We should also note that the results summarized in Figures 1 were obtained after numerous cycles of the electrode potential in both electrolytes during which the reconstruction was lifted and reformed and so the results shown are representative of true equilibrium conditions.

Of particular interest here are the dynamics of the potential-induced reconstruction in alkaline media with respect to acidic electrolyte. This information is assessed from a selected number of results showing the dependence of the X-ray scattering at two key reciprocal space positions as a function of potential, the so-called X-ray voltammetry (XRV). Figure 1c shows a representative results for the intensity dependence at the position of one of the rotated peaks in 0.1 M $HClO_4$ as well as the intensity dependence at the unrotated peak position in 0.1 M KOH. Figure 1b shows data for the same solutions obtained at (0, 0, 1.3), a position along the specular crystal truncation rods (CTR) where the reconstruction of the surface causes an increase in the scattered intensity due to the increased density of the surface layer. As illustrated in Figure 1c, due to the slow kinetics in the formation of the reconstructed surface, at the sweep rate used in these measurements (2.5 mV/s), there is considerable

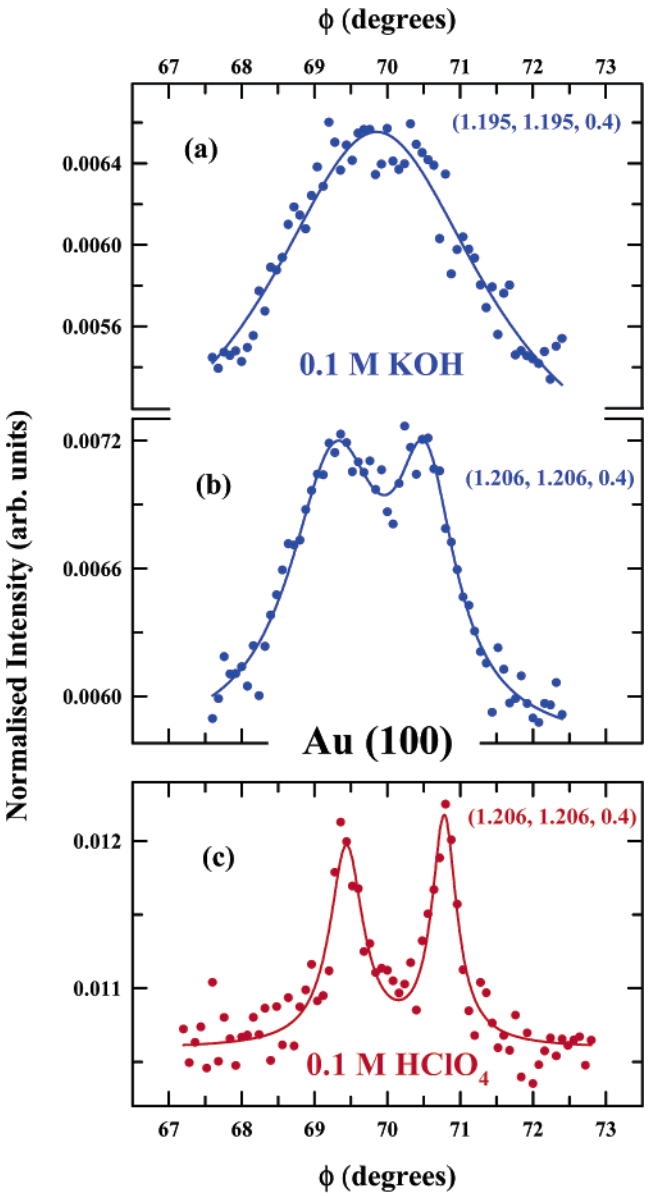

Figure 2. Rocking scans through (a) (1.195, 1.195, 0.4) and (b) (1.206, 1.206, 0.4) in 0.1 M KOH and (c) (1.206, 1.206, 0.4) in 0.1 M $HClO_4$. At these reciprocal space positions, scattering from the reconstructed "hex" phase is observed.

hysteresis as the potential is cycled. Previous kinetic studies have shown that the reconstruction forms over a time scale of 15−100 s.[11] The fact that in alkaline solution the data at the CTR position, Figure 1b, show the same hysteresis implies that in this environment the kinetics are controlled by the large-scale movement of the Au surface atoms rather than any local ordering effects, which is in accord with corresponding STM studies of Au(100) reconstruction.[9] Interestingly, in acid solution the shape of XRV curves at the (0, 0, 1.3) and (1.206, 1.206, 0.4) positions is completely different, i.e., while a reversible change in scattering intensity is observed at the specular CTR position, at the reconstruction position there is hysteresis as the potential is cycled. Given that the CTR is only sensitive to the density change at the surface it is reasonable to propose that although specific adsorption of anions acts to catalyze the mobility of gold surface atoms the formation of uniform "hex" domains is not enhanced by this movement. This observation is consistent with the STM results that the dynamics of

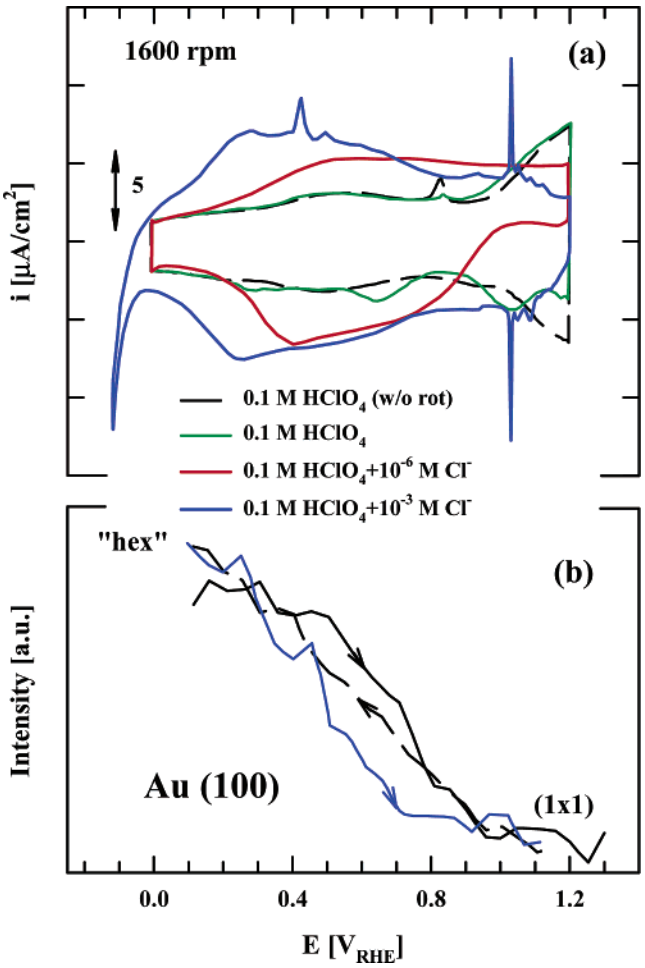

Figure 3. (a) CV's for the Au(100) electrode in pure 0.1 M $HClO_4$, with the addition of 10^{-6} M and 10^{-3} M Cl^- at 50 mV/s, (b) XRV measurements (2.5 mV/s) at (0, 0, 1.3), a position on the specular CTR, in 0.1 M $HClO_4$ and 0.1 M $HClO_4$ + 10^{-3} M Cl^-.

propagation of the reconstruction is faster in alkaline than in acid solution.[9]

The driving force for the transition from the reconstructed to (1 × 1) surface was proposed to be either an induced surface charge density[15] or adsorption/desorption of adsorbed species.[11;20] Considering that the adsorption of ions from supporting electrolyte is closely related to the charge distribution at the interface, it is very difficult to resolve this issue; for further details, readers are referred to specific reviews on reconstruction phenomena at metal−electrolyte interfaces.[20] Nevertheless, regardless of what triggers the reconstruction, it is obvious that the sharp lifting of the "hex" phase is controlled by specific adsorption of anions and the adsorption of hydroxyl species. To further probe the sensitivity of the "hex" ↔ (1 × 1) transition to the nature (coverage) of electrolyte anions, the surface coverage by adsorbates was controlled either directly, by addition of specifically adsorbing anions (Cl^-), or indirectly, by consuming the adsorbed species (OH_{ad}) in an electrochemical reaction in which strongly adsorbed OH is removed from the surface by a relatively weakly adsorbed reactant such as CO_{ad}.

3.2. Adsorbate-Induced Structure Changes. *3.2.1. Chloride Effect.* Close inspection of Figures 1b and 1c reveals that specific adsorption of anions (Cl^- and ClO_4) shifts the "equilibrium potential of the "hex" ↔ (1 × 1) transition to less positive values and can enhance the conversion dynamic (i.e., the steep lifting of the reconstruction in Figure 1c). To confirm that the presence of strong chemisorption can facilitate the "hex" ↔ (1 × 1) transition Cl^- was intentionally added into 0.1 M $HClO_4$: note that Cl^- is present as an impurity in perchloric acid at a concentration of at least 10^{-7} M,[18,19] In the SXS-EC measurements (Figure 3) there are two characteristics that represent the effect of Cl^-. The first is that even in the presence of 10^{-6} M Cl^- the pseudocapacitance in Figure 3a increases substantially, indicating that a true "double layer" does not exist on the Au(100) surface and that adsorption of anions indeed takes place at very low potentials. Adding 10^{-3} M Cl^- leads to both further increase in the pseudocapacitance and to the development of sharp peaks located at ≈0.4 V and ≈1.1 V. Using coulometry study, Lipkowski and co-workers showed that, in solution containing 10^{-3} M Cl^-, adsorption isotherm of chloride (Θ_{Cl}) on Au(111) exhibits the "S" shape, i.e., initially the anion surface concentration changes only slowly with potential then a step rise in Θ_{Cl} is observed, followed by a third regime of slow increase, where the adlayer packing density is close to saturation.[23] The S-shaped adsorption isotherm of Br^- is also observed for the Au(100)−Br_{ad} system,[24] indicating that potential-dependent surface coverage of halides on Au(*hkl*) follows similar adsorption isotherm. As shown by SXS, ordered adlayer structures on both Au(111) and Au(100) are formed in high coverage regime.[25] The second characteristic (shown in Figure 3b) is that the addition of 10^{-3} M Cl^- shifts the lifting of the reconstruction to less positive values, in agreement with the supposition that the "hex" ↔ (1 × 1) transition is triggered by specific adsorption of anions. The fact that Cl is strongly adsorbed on the Au(100) surface (even in "pure" perchloric acid) is important in explaining the strong pH effect in electrocatalysis of the ORR, as will be discussed in section 3.3.

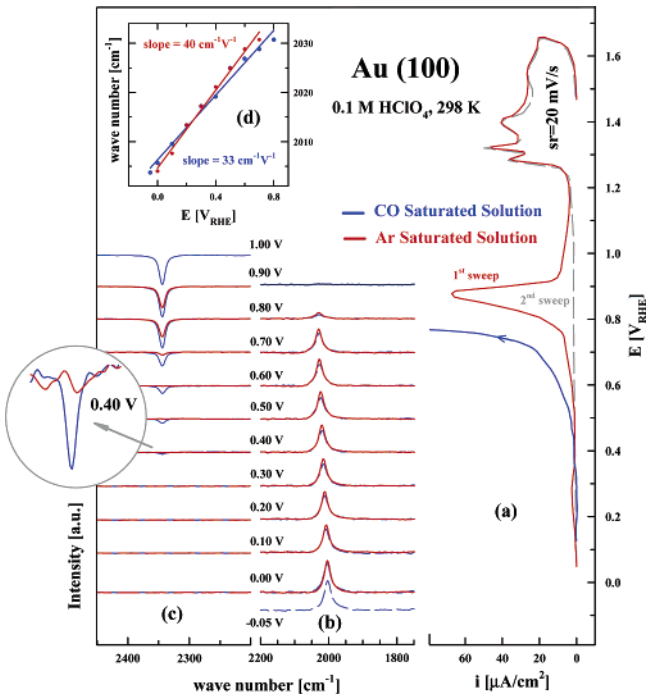

Figure 4. (a) CO stripping curve (50 mV/s) on Au(100) in Ar-purged 0.1 M $HClO_4$ solution and CO oxidation (50 mV/s) in CO-saturated 0.1 M $HClO_4$ solution; series of infrared spectra of adsorbed CO (b) and dissolved CO_2 (c) in Ar-purged 0.1 M $HClO_4$ solution at different potentials, insert of Figure 4c is magnification of the CO_2 bands at 0.4 V recorded in a solution free of CO (red curve) and in CO-saturated solutions (blue curve); (d) the Stark tuning slope for the CO_{ad} band.

3.2.2. CO Effect. The effect of CO on the thermodynamics and dynamics of the "hex" structure in KOH was previously studied by STM.[9] In contrast to the effect of anionic adsorbates such as hydroxide and Cl^- considered above, CO acts, quite

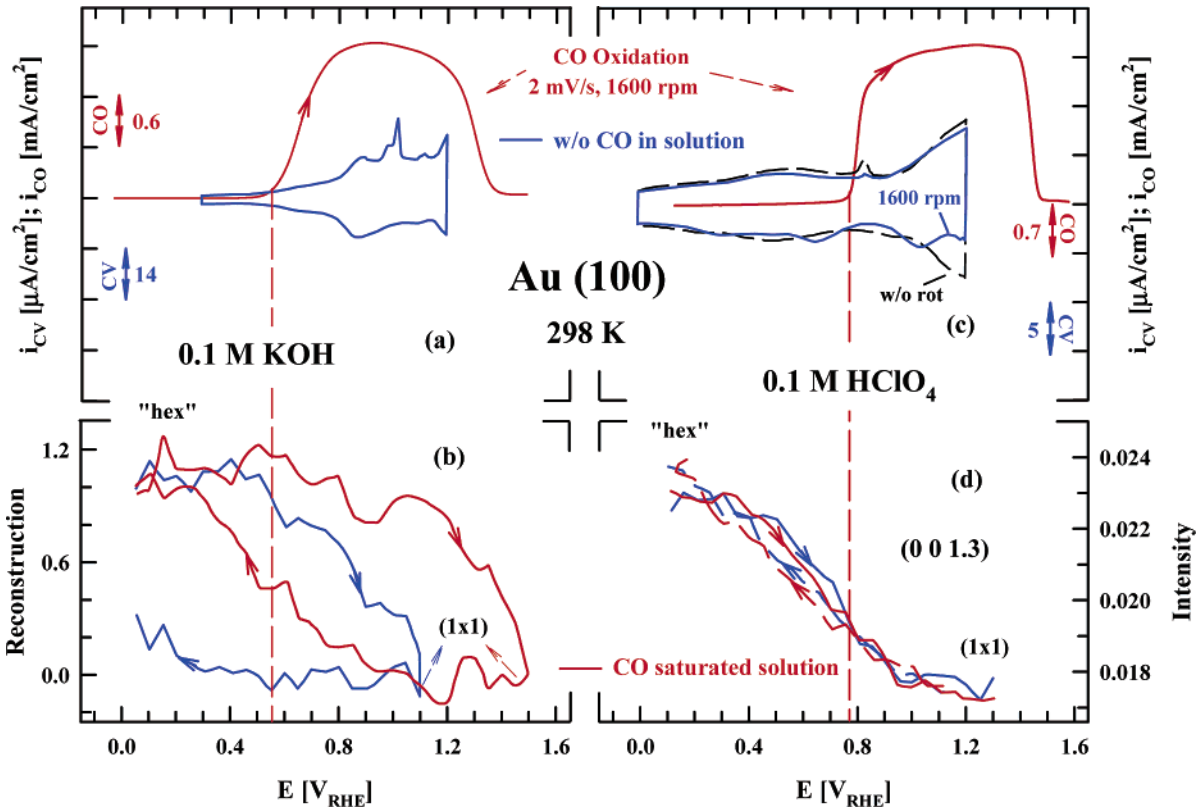

Figure 5. (a) The CV (50 mV/s) for a Au(100) electrode in 0.1 M KOH between 0 and 1.2 V along with a polarization curve for CO oxidation in CO-saturated 0.1 M KOH solution; (b) the "hex"-(1 × 1) reconstruction transition (2.5 mV/s) in 0.1 M KOH with and without CO added; (c) CV's (50 mV/s) in 0.1 M $HClO_4$ without rotation and at 1600 rpm, along with the polarization curve for CO oxidation in CO-saturated 0.1 M $HClO_4$ solution; (d) XRV measurements (2.5 mV/s) at (0, 0, 1.3), a position on the specular CTR, in 0.1 M $HClO_4$ without and with CO added to solution.

remarkably, to catalyze the formation of uniform "hex" domains. In this section, we report a complementary examination by SXS of the Au(100) reconstruction in both alkaline and acid solutions. Besides enabling a comparison to be made between the "hex" ↔ (1 × 1) transition in alkaline solution with respect to acidic media, the results shed light on the surface energetics of coadsorbed CO, OH_{ad}, and Cl_{ad}.

Figure 4a shows a representative CO stripping curve and CO oxidation current recorded in solution saturated (1 atm) with CO. To ensure the complete poisoning of the electrode surface with CO prior to recording the oxidation currents, the electrode potential was held at 0.0 V (the immersion potential) for 5 min at a rotation rate of 2500 rpm. To emphasize the onset of CO oxidation, only a part of the CO polarization curve is shown; polarization curves for CO oxidation over a wide potential region are shown in Figure 5. For the anodic stripping voltammetry CO is adsorbed in CO-saturated solution followed by purging the solution with Ar. Upon sweeping the potential positively from 0.0 V the onset of CO oxidation commences at ca. 0.65 V, forming first the pre-ignition wave over the potential range of 0.65 V−0.8 V. Above 0.8 V the stripping voltammogram is characterized by a sharp peak centered at 0.9 V. The charge under the stripping peak is ca. 370 $\mu C/cm^2$, indicating that almost a full monolayer of CO is adsorbed on the surface. The assessed charge is much higher than the fractional coverage (ca. 0.1 ML) extracted from the quantity of CO_2 produced upon CO electrooxidation on Au(210).[26,27] Rather than debate these differences, the interested reader is referred to the original references for details. The successive negative going sweep and the second cycle traced accurately the base voltammogram of clean Au(100), attesting to the complete removal of CO from solution by Ar. The binding site occupancy of CO on Au(100) and the onset of CO oxidation (the production of CO_2) under the same experimental conditions are established by FTIR. A relatively weak, yet readily discernible, C−O stretch is observed at 2001−2030 cm^{-1}. This feature is consistent with the presence of bridge-bonded CO (i.e., coordinated to two gold atoms). The Stark tuning slope of 40 cm^{-1} V^{-1} is also depicted in Figure 4d. To the best of our knowledge, the potential-dependent surface infrared spectra for CO on Au(100) in $HClO_4$ have not been reported previously. Figure 4c shows that oxidative removal of CO from the Au(100) surface, established by monitoring the concomitant development of O−C−O stretch of dissolved CO_2 at 2343 cm^{-1}, starts at 0.7 V. Clearly, the decrease in the CO intensity at $E = 0.7$ V is mirrored by the onset of adsorption of OH on gold polycrystalline electrode in 0.l M $HClO_4$ [17,28] and appearance in CO_2 production in Figure 4c, consistent with the Langmuir−Hinshelwood (L−H) mechanism for CO oxidation, i.e.,

$$CO_{ad} + OH_{ad} = CO_2 + H^+ + e^- \qquad (1)$$

Further insight into the CO oxidation reaction was obtained by close inspection of the onset potential for CO stripping with respect to bulk oxidation. Two examples illustrated in Figure 4 show that the onset potential for pure CO oxidation (CO_2 production in Figure 4c and the current for CO oxidation in Figure 4a) is shifted negatively by ca. 0.3 V with respect to the stripping curve, consistent with the positive reaction order. Closely following our discussion for electrooxidation of CO on Pt(*hkl*),[1] we propose that in CO-saturated solution a high surface coverage state of CO, which is created by the "crowding" of the surface with CO that reduces its adsorption energy via CO−CO repulsion, is more reactive than relaxed CO layer created

in CO stripping experiments. Therefore, even for the same coverage of OH, the closely packed CO adlayer is more reactive than the relaxed state, and thus is oxidized from the surface at lower potentials. Notice that the rate of reaction 1 at low overpotentials is very low (from Figure 4a, @0.5 V ca. 10μA/cm^2), suggesting that the surface coverage by oxygenated species between $0.4 < E < 0.7$ V is indeed small. Nevertheless, these results indicate that the real onset potential for OH adsorption is at 0.4 V rather than at 0.7 V, as determined by surface-enhanced Raman scattering measurements.[17,28] The same effect is observed in alkaline solution (results not shown), suggesting that the sign of reaction order of CO oxidation on Au(100) is pH-independent. Edens et al. found the kinetics of CO oxidation display essentially a first-order dependence in CO.[29]

The kinetics of CO oxidation are, however, strongly pH dependent, as demonstrated in Figure 5. A notable feature is that the kinetics in alkaline solution (Figure 5a) are faster than in acid media (Figure 5c). If the L−H mechanism is operative, higher catalytic activity in the alkaline solution (evidenced by the lower CO oxidation onset potential, which is in Figure 5 marked with dashed red lines) implies that the surface coverage by OH is larger in alkaline than in acid solution. In acid solution, where there is strong competition between OH and anions for the Au sites, the surface coverage by OH is significantly reduced with respect to alkaline solution and thus the kinetics of reaction 1 is strongly inhibited at low pH. The explanation, therefore, for the remarkable effect of pH on the rate of CO oxidation on Au(100) is the "pH-dependent" adsorption of OH. At this point it is appropriate to note that other research groups have proposed different models for the pH-dependent kinetics of CO on Au(*hkl*) surfaces. For example, in analogy with CO oxidation in homogeneous solutions, Weaver and co-workers suggested that pH-dependent kinetics behavior is consistent with a reaction pathway featuring the involvement of an adsorbed hydroxycarbonyl intermediate. While at higher pH values hydroxylcarbonyl is formed by OH^- discharge onto adsorbed CO sites, at lower pH water rather than OH^- is becoming the preferred reactant. Again, rather than debate interpretation here, the interested reader is referred to the original reference for details.[29]

In the previous STM study it was found that the presence of adsorbed CO can alter the potential-dependent thermodynamics (shifts the "hex" ↔ (1 × 1) transition positively) as well as the dynamics (the "hex" phase develops rapidly) of Au(100) reconstruction.[9] Parallel electrochemical (Figure 5a) and SXS (Figure 5b) measurements support directly the involvement of adsorbed CO in this surprising phenomenon. As discussed above, in alkaline solution free of CO, a reproducible XRV at the (1.206, 1.206, 0.4) position was obtained after five cycles of the electrode potential (a sweep rate of 2.5 mV/s) between $0 < E < 1.2$ V. Notice that the surface reconstruction of Au(100) starts as low as at 0.5 V. Figure 5a shows cyclic voltammograms obtained under similar conditions, but in the electrochemical cell. The first sweep recorded with 50 mV/s shows a characteristic shoulder at 0.9 V which is followed with a sharp peak appearing at about 1.0 V during the positive going sweep. This peak was suggested to be a fingerprint for the potential-induced lifting of the reconstruction,[9] by analogy with related peaks observed in acidic media.[20] Given that at 1.0 V the surface is already half reconstructed, it appears that although there is no *direct* correlation between the sharp peak and the *onset* of surface reconstruction the pseudocapacitance feature at 1.0 V is indeed associated with the "hex" ↔ (1 × 1) transition. Further analysis of the XRV−CV results unambiguously shows that the "hex" ↔ (1 × 1) transition is triggered by the appearance of pseudocapacitance at 0.5 V, which most likely corresponds to an OH_{ad} layer formation on the "hex" surface. This supposition is plausible since the onset of CO oxidation on this surface (Figure 5a) coincides with the formation of this pseudocapacitance. At more positive potentials the rate of CO oxidation increases sharply reaching a diffusion limited value at 0.8 V, which above 1.25 V is attenuated rapidly due to significant oxide formation. Further inspection of Figures 5a and 5b reveals that the addition of CO leads to a significant (ca. 0.3 V) positive shift in the thermodynamic potential for the "hex" ↔ (1 × 1) transition. In agreement with the STM results, SXS measurements confirm that adsorbed CO on Au(100) in alkaline solution indeed acts to catalyze the formation of uniform hexagonal domains. This observation is notable in that the adsorption of CO on Pt(100) in a vacuum is known to "lift" the hex phase.[30] To rationalize this apparently opposite behavior we have previously suggested that the nature of the driving force responsible for the enhanced reconstruction of Au(100) in the presence of CO is an increase in the potential of zero charge for Au(100) upon CO adsorption. Alternatively, a more plausible explanation is that the continuous removal of OH_{ad} in the L−H reaction may in fact stabilize the "hex" phase over a much wider potential range than in CO-free alkaline solution. Such a mechanism would correlate nicely with the weak adsorption of CO on Au surfaces,[31] i.e., the Au(100)−OH interaction is much stronger than the Au(100)−CO interaction. The weak interaction of CO with gold is well established at the gold−gas interface;[32] it is found that although oxidation to form CO_2 does proceed at room temperature, CO exhibits only very weak adsorption.

In acid solution, however, CO has negligible effect on the potential range of thermodynamic stability of the "hex" ↔ (1 × 1) transition, i.e., in Figure 5d XRVs at the (0, 0, 1.3) position are almost the same in solution with or without dissolved CO. These results provide very important information on the energetics of the Au(100)−adsorbate interaction and also help to develop an understanding of quite intriguing promotion of the reconstruction in alkaline solution saturated with CO. The fact that the thermodynamic and dynamic properties of the "hex" phase are unaffected by adsorbed CO are in agreement with a weak Au(100)−CO interaction. Furthermore, previous suggestions that the increase of potential of zero charge induced by CO adsorption in alkaline solution is responsible for the enhanced formation of "hex" domains [9] is not plausible since no change in the nature of the "hex" ↔ (1 × 1) transition is observed in Figure 5d, although CO is indeed adsorbed on the Au(100) surface (as shown in Figure 4). On what basis, then, can apparent opposite behavior observed for the "hex" ↔ (1 × 1) transition in acid versus alkaline electrolytes be rationalized? One relevant factor is that in contrast to alkaline solution the kinetics of the L−H reaction in acidic media are not governed only by the surface concentration of CO_{ad} and OH_{ad}, but also are strongly affected by a delicate balance between the coverage of CO_{ad}, OH_{ad}, and a third party (spectator) species, viz., the anions from supporting electrolytes.[33] In alkaline solution, OH^- anions are both *reactant* and spectator species, the latter being OH_{ad} which is not consumed in reaction 1. In acid solution at low overpotentials OH is most likely replaced from the active sites by specifically adsorbing anions (ClO_4^-, Cl^-) and thus the onset potential for the oxidation of CO in 0.1 M $HClO_4$ (Figure 5c) is shifted ca. 0.2 V positively from that observed in 0.1 M KOH (Figure 5a). In accord with the kinetics of CO oxidation, the pronounced pH effect on the surface reconstruction of Au(100) in solution containing CO can be understood

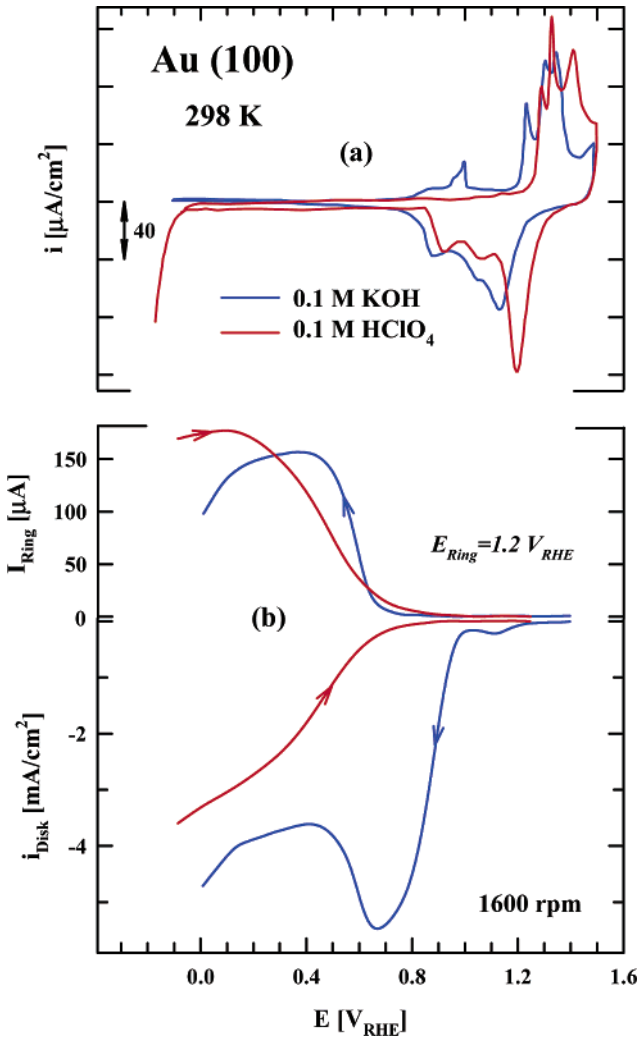

Figure 6. (a) CV's for the Au(100) electrode in 0.1 M $HClO_4$ and 0.1 M KOH, (b) ORR (bottom part) and peroxide oxidation (upper part) currents in the same solutions at 1600 rpm. Sweep rate (50 mV/s).

as a pH-dependent surface coverage by anionic species. While in alkaline solution the "hex" ↔ (1 × 1) transition is determined exclusively by surface coverage of OH_{ad}, in acid solution the equilibrium potential for this transition is controlled by the surface coverage of ClO_4^- and Cl^-, as well as that of OH^-. Taking into account that specifically adsorbing anions *cannot* be displaced by CO from the Au(100) surface, i.e., the Au−CO interaction is weaker than the Au−Cl_{ad} interaction, the absence of CO effects on the restructuring may well be attributed to high surface coverage with ClO_4^- and Cl^- even at relatively low potentials. This, in turn, will have a considerable effect on the pH-dependent kinetics of the ORR.

3.3. ORR on Au(100) in $HClO_4$ and KOH: Origin of the pH Effect. The electrochemical reduction of oxygen and hydrogen peroxide on gold single-crystal electrodes are typical reactions that show both a pronounced pH effect as well as a considerable structure sensitivity.[2] Figures 6a and 6b show the voltammetry of Au(100) in oxygen-free 0.1 M $HClO_4$ and 0.1 M KOH solutions (a) and, correspondingly, the ring-disk kinetic data for the ORR (b). The Levich plots, summarized in Figure 7a, yield straight lines with intercepts corresponding to the kinetic currents, in acid solution at 0.46 V, $i_k = 2.74$ mA cm^{-2} and in alkaline solution, at 0.8 V, $i_k = 10.93$ mA cm^{-2}. The slope of the straight lines, "the so-called B factor", allows one to assess the number of electrons involved in the ORR. The

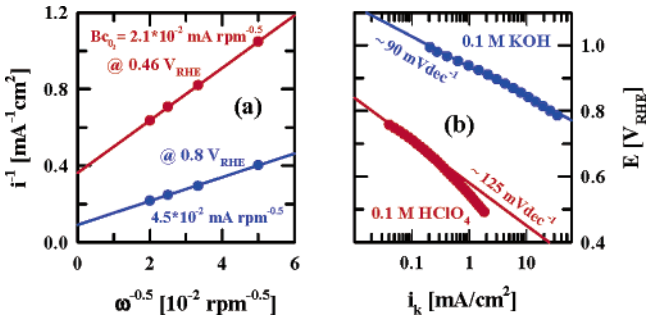

Figure 7. (a) Levich-Koutezki plots, (b) Tafel slopes extracted from the polarization curves in Figure 6.

experimental values of $Bc_0 = 2.1 \times 10^{-2}$ mA rpm$^{-0.5}$ in acid and $Bc_0 = 4.5 \times 10^{-2}$ mA rpm$^{-0.5}$ in alkaline solution, evaluated from Figure 7a, agree well with the theoretical values of $Bc_0 = 2.2 \times 10^{-2}$ mA rpm^{-05} and $Bc_0 = 4.4 \times 10^{-2}$ mA rpm^{-05} for $2e^-$ and $4e^-$ reduction, respectively, using literature data for O_2 solubility, viscosity, and oxygen diffusion.[34,35] Figure 7b shows the Tafel plots of mass transport corrected currents at Au(100) in both electrolytes. Depending on the fitting method, i.e., the method of drawing the tangent through the points of what appear to be continuous curve, one might extrapolate any Tafel slope between 85 and 135 mV dec^{-1} In our case−we somewhat arbitrarily fitted the curves with a single slope of ca. 125 mV dec^{-1} in acid solution and ca. 90 mV dec^{-1} in alkaline solution. On the basis of these values we suggest that the transfer of the first electron is the rate-determining step in both electrolytes. Notice, however, for the first electron transfer as the rate-determining step the "ideal" Tafel slope at 298 K should be 118 V dec^{-1}. Further analysis of Figure 7b shows a large variation in activity between these two electrolytes, with the activity in $HClO_4$ solution being nearly 4 orders of magnitude lower than in KOH at the same potential vs RHE. Despite considerable effort by many research groups to determine the origin of these differences, the reason for this remarkable pH-sensitivity remains unclear. In the following discussion we demonstrate that the key to understanding the oxygen reduction kinetics at the Au−liquid interface is to be found in understanding the interplay between the energetic properties of the substrate and the ability of *metal* surface atoms to adsorb molecular O_2 and the reaction intermediates. Kinetic data assessed from Figures 6 and 7 revealed that a series pathway via an peroxide intermediate formation is operative for the ORR on Au(100) in the entire pH range, i.e.,

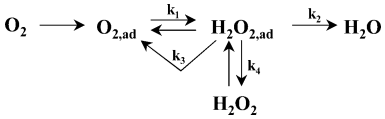

This reaction scheme can be considered as a special case of the general mechanism in which there is no splitting of the O−O bond before a peroxide species is formed.[1] Peroxide, on the other hand, may or may not be further reduced to water. In either case, the rate-determining step appears to be the addition of the first electron to O_2,

$$O_2 + e^- = O_{2,ad}^- \quad (E^\circ = -0.3\ \mathrm{V} + \Delta G_{ad}/F \text{ vs. SHE}) \qquad (2)$$

The rate expression is then,[1]

$$i = nFKc_{O2}(1 - y\Theta_{ad})^x \exp(-\beta FE/RT) \exp(-\Delta G_\theta^*/RT) \qquad (3)$$

where i is the observed current, n is the number of electrons, K is the rate constant, c_{O_2} is the concentration of O_2 in the solution, Θ_{ad} is the total surface coverage by anions (Θ_{anions}) and OH_{ad} ($\Theta_{OH_{ad}}$), x is the order of activity of Au sites, y is the number of Au sites blocked by spectator species, E is the applied potential, ΔG_θ^* is the standard activation energy ($\Delta G_\theta^* = \Delta G_0^* + \gamma r \Theta_{ad}$), β and γ are the symmetry factors (assumed to be 1/2), and r is a parameter characterizing the rate of change of the apparent standard free energy of adsorption with the surface coverage by adsorbing species. In deriving eq 3, it is assumed that the reactive intermediates, $(O_2^-)_{ad}$ and $(HO_2^-)_{ad}$, are adsorbed only to low coverage, i.e., they are not a significant part of Θ_{ad}. In the following sections, this reaction pathway and rate expression are used to analyze the effects of various factors on the kinetics of the ORR on the Au(100) surface.

3.3.1. Energetic Effects: The ΔG Term. Most available experimental data concerned with the heats of adsorption of oxygen on metal surfaces has unambiguously showed that in UHV molecular oxygen does not spontaneously chemisorb on gold single crystals.[36−38] How is it then possible to have even a $2e^-$ reduction on Au(*hkl*) surfaces in electrolyte? Very recently, we used a computational approach in order to assess the quantum chemical nature of the adsorption O_2 and O_2^- on a single Au atom, simulating O_2 adsorption in reaction 2.[39] These density functional theory (DFT) calculations have provided invaluable information to complement and correctly interpret experimental data. For instance, by closely examining the evolution of the molecular orbital character as O_2 and O_2^- approaches the Au atom it was found that while O_2 does *not* interact with Au, the superoxide radical anion O_2^- interacts weakly with Au. Even though the adsorption energy of O_2^- on Au is weak and slightly positive ($\Delta G = 0.25$ eV), it was evident from the energy correlation diagram and the molecular orbital diagram that there exists some interaction through the Au $5d_{xy}$ and O_2^- 2π in the form of a polarization or image charge.[39] Extending this phenomenon to reaction 2, it appears that the first electron transfer and the formation of the O_2^- state must be an inner sphere reaction where an interaction energy between both the neutral O_2 molecule (the initial physisorbed state) and the O_2^- anion (the final weakly chemisorbed state) leads to an *adsorbed* intermediate state with the energy of adsorption (the ΔG term in eq 3) which may affect the reversible potential for the rate-determining step in eq 2. These findings may indeed provide the answer to the above question: Au can reduce O_2 to peroxide and/or OH^- simply because the chemisorbed species is not O_2 but rather O_2^-. Note that because H^+ is not involved in the rate-determining step, the rate of reaction 2 will not depend on pH. The reactions following the rate-determining step, however, e.g., protonation to form peroxide, are pH dependent, but as long as reaction 2 is the rate-determining step the reversible potential for reaction 2 will be pH independent. This is illustrated more graphically in the modified Pourbaix diagram for hydrogen peroxide in Figure 8. Hence, because of the overlap in the equilibrium potentials of peroxide and superoxide at pH = 14, no strong interaction of O_2^- with Au(100) is required and thus the surface reduces oxygen to either peroxide or OH^- (Figure 6). At pH = 0 the overpotential is very large, increased by essentially 0.059×14 V ≈ 0.94 V because the thermodynamic potential has shifted by 0.84 V positively but the reversible potential for the rate-determining step (eq 2) has not. Therefore, at pH = 0 only surfaces with strong chemical interaction of O_2^- (viz., Pt-group metals) can reduce oxygen to peroxide and even stronger interaction is needed to reduce oxygen to water at low overpotentials. Clearly, the Au(100)−

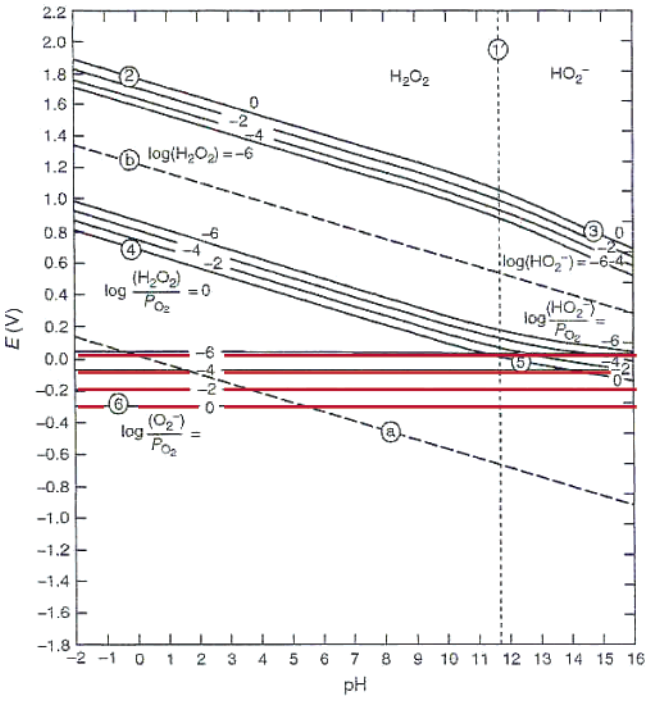

Figure 8. Modified Pourbaix diagram for hydrogen peroxide with the equilibria for the superoxide/oxygen reaction (labeled 6 in the diagram) added. Other notations for equilibria as in ref 41.

O_2^- energetics are too weak to break the O−O bond in acid solution and the ORR in 0.1 M $HClO_4$ follows the serial pathway in which the final product is H_2O_2 (Figure 6). It is important to emphasize, however, that in real systems the ORR proceeds not on pure metal surfaces but rather on a metal electrode which is modified with coadsorbed anions, water and hydroxyl species. Bearing this in mind, the present (admittedly simplified) approach appears to capture only a part of the origin of the pH effects. Therefore, to fully unravel the puzzle of the pH-dependent kinetics of the ORR on Au(100) it is necessary to further analyze the pH-dependent adsorption of spectator species and the contribution of $(1 - \Theta_{ad})$ term to the pH effects.

3.3.2. Anion Effects: The $(1 - \Theta_{ad})$ Term. It is now well established that the kinetics of hydrogen reaction and the oxidation of CO on metal electrodes are pH-dependent processes.[1] From carefully selected experiments, we have recently presented an argument that the pH-dependent kinetics of these two reactions on Pt may, in part, arise from the pH-dependent adsorption of hydroxyl species and specifically adsorbing anions, i.e., from the $(1 - \Theta_{ad})$ term in eq 3. Along the same lines, we will demonstrate that the $(1 - \Theta_{ad})$ term may indeed play a very important role in the pH-dependent kinetics of the ORR on Au(100). In 0.1 M $HClO_4$, Θ_{ad} is determined by the surface coverage of OH_{ad} (Θ_{OH}), specifically adsorbed perchlorate anions (Θ_{ClO_4}), and specifically adsorbed chloride anions ($\Theta_{Cl\,ad}$), i.e., ($\Theta_{ad} = \Theta_{OH_{ad}} + \Theta_{ClO_4} + \Theta_{Cl_{ad}}$). In 0.1 M KOH, however, Θ_{ad} is determined exclusively by the surface coverage of hydroxyl species, i.e., $\Theta_{ad} = \Theta_{OH}$. In section 3.2.2, we used the CO oxidation reaction as a probe to determine the onset of OH adsorption. Surprisingly, it was found that OH is indeed adsorbed at rather low potentials in both alkaline as well as acid media. Given that the surface coverage by OH is higher in the former media it was suggested that OH adsorption in $HClO_4$ is always in competition with adsorption of ClO_4^- and Cl^-. This competitive adsorption has an important and generally adverse effect on the adsorption of O_2 and the formation of active intermediates and, thus, on the pH-dependent kinetics of

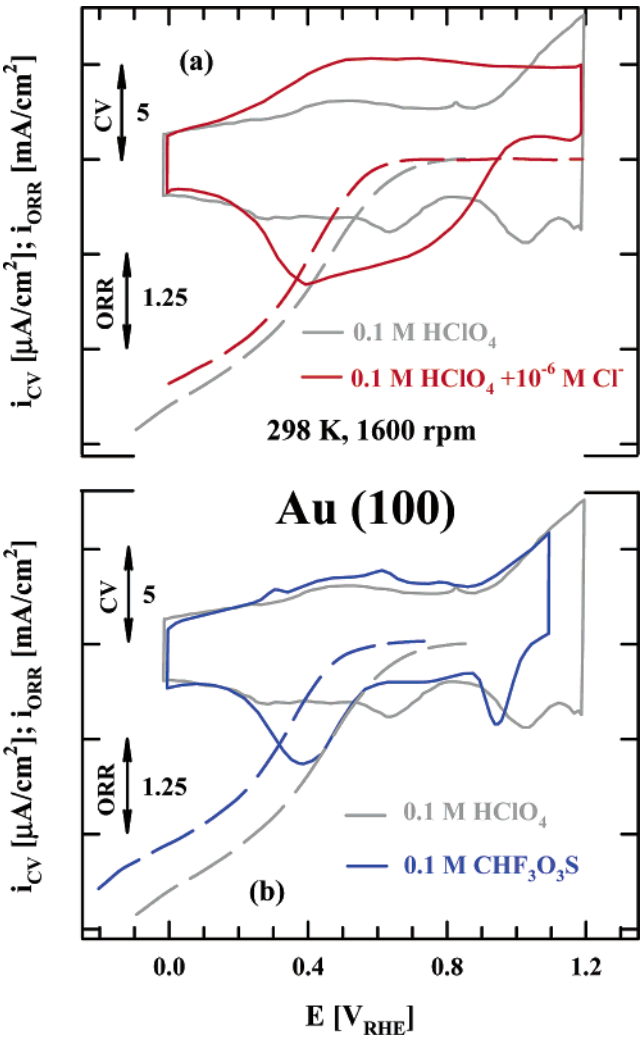

Figure 9. (a) CV's in 0.1 M $HClO_4$ and in 0.1 M $HClO_4$ + 10^{-6} M Cl^-, with corresponding ORR polarization curves obtained at 1600 rpm, (b) the CV's in 0.1 M CHF_3O_3S and 0.1 M $HClO_4$ (added for comparison) with ORR polarization curves. Sweep rate (50 mV/s)

the ORR. As illustrated in Figure 6, in 0.1 M KOH the ORR reaction occurs concurrently with the reduction of the hydroxyl layer. In 0.1 M $HClO_4$, however, desorption of OH_{ad} is accompanied with simultaneous adsorption of ClO_4^- and Cl^- anions, which in turn will block the active metal sites required for the rate-determining step to occur; so the kinetics of reaction 3 is controlled through the $(1 - \Theta_{ad})$ term. Additional evidence that the kinetics in $HClO_4$ is controlled by the surface coverage of Cl_{ad} can be found in Figure 9. Figure 9a shows that the ORR on the Au(100) surface in 0.1 M $HClO_4$ +10^{-6} M Cl^- is inhibited, with the activity in solution containing Cl^- being ca. 2 times less than in 0.1 M $HClO_4$. This is in line with the secondary structure sensitivity observed in gas-phase catalysis, where some secondary process in the reaction mechanism leads to site blocking.

To avoid specific adsorption of anions the ORR was also performed in a so-called "nonadsorbing" electrolyte such as trifluoromethane sulfonic acid (CF_3SO_3H). The cyclic voltammogram along with the polarization curve for the ORR on Au(100) in 0.1 M CF_3SO_3H is shown in Figure 9b and compared with the corresponding results in $HClO_4$. Surprisingly, the ORR in "non-adsorbing" electrolyte is inhibited even more than in $HClO_4$ containing 10^{-6} M Cl^-, with an activity in 0.1 M CF_3SO_3H electrolyte being ca. 5 times lower than in 0.1 M $HClO_4$ (Figure 10b). The results for the ORR reaction, therefore,

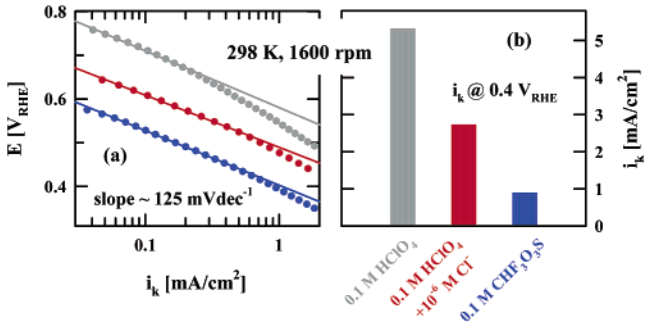

Figure 10. (a) Tafel slopes extracted from polarization curves for ORR from (Figure 9a) and (Figure 9b), (b) kinetic currents (corrected for diffusion) for ORR at 0.4 V.

suggest that even in "ultrapure" CHF_3O_3S solution Cl^- is present at a trace level ($<10^{-6}$ M). This is clear from the cyclic voltammetry of Au(100) in CHF_3O_3S, which shows a rather sharp peak at 0.4 V for Cl_{ad}, as would be seen for Cl_{ad}. Finally, we note that the percentage of peroxide produced during the ORR (not shown) in all three electrolytes is the same and is close to 100%. Additionally, a single Tafel slope of ca. 125 mV/dec (Figure 10a), inferred from current densities corrected for diffusion resistance, are observed irrespectively of the nature of solution. As discussed before, this Tafel slope is characteristic for the first charge-transfer step as the rds (eq 2) under Langmurian conditions of adsorption of O_2^- and reaction intermediates.[40] Taken together, it is reasonable to suggest that in all three electrolytes the reaction mechanism of the ORR on Au(100) is the same ("serial" $2e^-$ reduction pathway) and that the kinetic differences are contained in the preexponential $(1 - \Theta_{ad})$ term.

4. Conclusions

The effects of pH on the surface reconstruction of Au(100), on CO oxidation, and on the oxygen reduction reaction (ORR) have been studied by a combination of SXS, FTIR spectroscopy, and RRDE measurements. In agreement with previous SXS and STM results, the potential induced "hex" ↔ (1×1) transition occurs faster in an alkaline electrolyte than in weakly adsorbing acidic media. In alkaline solution CO adsorption facilitates the formation of a "hex" phase because the continuous removal of OH_{ad} in the L−H reaction may in fact stabilize the "hex" phase over a much wider potential range than in CO-free alkaline solution. Such a mechanism correlates nicely with a weak Au−CO interaction, i.e., the Au(100)−OH interaction is stronger than Au(100)−CO interaction.

In acid solution, however, CO has negligible effect on the potential range of thermodynamic stability of the "hex" ↔ (1×1) transition. The apparent opposite behavior observed for the "hex" ↔ (1×1) transition in acid versus alkaline electrolyte was rationalized by the fact that in contrast to alkaline solution, the kinetics of the L−H reaction in acidic media are not governed only by the surface concentration of CO_{ad} and OH_{ad}, but also are strongly affected by the delicate balance between the coverage of CO_{ad}, OH_{ad}, and a third party (spectator) species, viz., the anions from supporting electrolytes. While in alkaline solution the "hex" ↔ (1×1) transition is determined exclusively by surface coverage of OH_{ad} in acid solution, the equilibrium potential for this transition is controlled by the surface coverage of ClO_4^- and Cl^- as well as that of OH. Taking into account that specifically adsorbing anions *cannot* be displaced by CO from the Au(100) surface, i.e., the Au−CO interaction is weaker than the Au−Cl_{ad} interaction, the absence of CO effects on the

restructuring in acid solution is attributed to a high surface coverage with spectator species even at relatively low potentials.

Finally, we propose that the puzzling pH-dependent kinetics of the ORR on Au(100) can be understood by discussing the relationships between the kinetic rates and two terms: (i) the energetic ΔG term, which is determined by the energetics of the Au(100)$-O_2^-$ interaction and is controlling the value of the reversible potential for the rate-determining step $O_2 + e = O_2^-$, and (ii) the preexponential $(1 - \Theta_{ad})$ term which is controlling the availability of active sites for the adsorption of O_2^- and the reaction intermediates.

Acknowledgment. This work was supported by the Director, Office of Science, Office of Basic Energy Sciences, Division of Materials Sciences, US DOE, under Contract No. DE-AC03-76SF00098. C.A.L. acknowledges the support of an EPSRC Advanced Research Fellowship, and M.E.G. acknowledges the support of an EPSRC studentship. The SXS measurements were performed at SSRL which is funded by the Division of Chemical Sciences (DCS), US DOE. M.A. acknowledges the Humboldt Foundation for a Feodor Lynen Fellowship.

References and Notes

(1) Marković, N. M.; Ross, P. N. *Surf. Sci. Rep.* **2002**, *45*, 121−254.
(2) Adzic, R. R. *Electrocatalysis*; Wiley-VCH: New York, 1998; pp 197−242.
(3) Adzic, R. R.; Marković, N. M.; Vesovic, V. B. *J. Electroanal. Chem.* **1984**, *165*, 105−120.
(4) Marković, N. M.; Adzic, R. R.; Vesovic, V. B. *J. Electroanal. Chem.* **1984**, *165*, 121−133.
(5) McIntyre, J. D. E.; Peck, W. F. *Electrochemistry at single-crystal metal electrodes. Electrocatalytic effects on surface atomic structure, defects and adatoms on oxygen reduction*; The Electrochemical Society: Pennington, NJ, 1984; pp 102−130.
(6) Taylor, E. J.; Vilambi, N. R. K.; Gelb, A. *J. Electrochem. Soc.* **2003**, *136*, 1939−1944.
(7) Strbac, S.; Adzic, R. R. *Electrochim. Acta* **1996**, *41*, 2903−2908.
(8) Marković, N. M.; Tidswell, I. M.; Ross, P. N. *Langmuir* **1994**, *10*, 1−4.
(9) Edens, G. J.; Gao, X.; Weaver, M. J.; Marković, N. M.; Ross, P. N. *Surf. Sci. Lett.* **1994**, *302*, L275−L282.
(10) Schmidt, T. J.; Stamenkovic, V.; Arenz, M.; Marković, N. M.; Ross, P. N. *Electrochim. Acta* **2002**, *47*, 3765−3776.
(11) Tidswell, I. M.; Marković, N. M.; Lucas, C.; Ross, P. N. *Phys. Rev. B* **1993**, *47*, 16542.
(12) Lucas, C.; Marković, N. M.; Ross, P. N. *Surf. Sci.* **1996**, *340*, L949−L954.
(13) Lucas, C.; Marković, N. M.; Ross, P. N. *Phys. Rev. Lett.* **1996**, *77*, 4922−4925.
(14) Lucas, C. A.; Marković, N. M.; Grgur, B. N.; Ross, P. N., Jr. *Surf. Sci.* **2000**, *448*, 65−76.
(15) Ocko, B. M.; Wang, J.; Davenport, A.; Isaacs, H. *Phys. Rev. Lett.* **1990**, *65*, 1466−1469.
(16) Ataka, K.; Yotsuyanagi, T.; Osawa, M. *J. Phys. Chem.* **2003**, *100*, 10664−10672.
(17) Li, X.; Gewirth, A. A. *J. Am. Chem. Soc.* **2003**, *125*, 7080−7099.
(18) Marković, N. M.; Hanson, M.; McDougal, G.; Yeager, E. *J. Electroanal. Chem.* **1986**, *241*, 309.
(19) Marković, N. M.; Ross, P. N. *J. Electroanal. Chem.* **1992**, *330*, 499−520.
(20) Kolb, D. M. *Prog. Surf. Sci.* **1996**, *51*, 109−173.
(21) Gao, X.; Hamelin, A.; Weaver, M. J. *Phys. Rev. Lett.* **1991**, *67*, 6993.
(22) Gao, X.; Hamelin, A.; Weaver, M. J. *Surf. Sci. Lett.* **1992**, *274*, L588.
(23) Lipkowski, J.; Shi, Z.; Chen, A.; Pettinger, B.; Bilger, C. *Electrochim. Acta* **1998**, *43*, 2875.
(24) Blizanac, B. B.; Arenz, M.; Gallagher, M.; Lucas, C.; Ross, P. N.; Marković, N. M. *J. Phys. Chem.*, in preparation.
(25) Magnussen, O. M. *Chem. Rev.* **2002**, *102*, 679−725.
(26) Chang, S.-L.; Hamelin, A.; Weaver, M. J. *Surf. Sci. Lett.* **1990**, *239*, L543−L547.
(27) Chang, S.-L.; Hamelin, A.; Weaver, M. J. *J. Phys. Chem.* **1991**, *95*, 5560−5567.
(28) Zou, S.; Zemlyanov, E. R.; Weaver, M. J. *Langmuir* **2003**, *16*, 745−763.
(29) Edens, G. J.; Hamelin, A.; Weaver, M. J. *J. Phys. Chem.* **1996**, *100*, 2322−2329.
(30) Somorjai, G. A.; Van Hove, M. A. *Prog. Surf. Sci.* **1989**, *30*, 201.
(31) Somorjai, G. A. *Introduction to Surface Chemistry and Catalysis*; John Wiley & Sons: New York, 1993.
(32) Gottfried, J. M.; Schmidt, K. J.; Schroeder, S. L. M.; Christmann, K. *Surf. Sci.* **2003**, *536*, 206−224.
(33) Marković, N. M.; Lucas, C. A.; Rodes, A.; Stamenkovic, V.; Ross, P. N. *Surf. Sci. Lett.* **2002**, *499*, L149−L158.
(34) Marković, N. M.; Gasteiger, H. A.; Ross, P. N. *J. Phys. Chem.* **1995**, *99*, 3411−3415.
(35) Marković, N. M.; Lucas, C. A.; Gasteiger, H. A.; Ross, P. N. *Surf. Sci.* **1996**, *365*, 229−240.
(36) Chesters, M. A.; Somorjai, G. A. *Surf. Sci.* **1975**, *52*, 21−28.
(37) Canning, N. D. S.; Outka, D.; Madix, R. J. *Surf. Sci.* **1984**, *141*, 240−254.
(38) Gottfried, J. M.; Schmidt, K. J.; Schroeder, S. L. M.; Christmann, K. *Surf. Sci.* **2002**, *511*, 65−82.
(39) Zhuang, G.; Marković, N. M.; Ross, P. N. *Quantum chemical modeling of the electrochemical reduction of oxygen*, 1st ed.; Electrochemical Society: Pennington, NJ, in press.
(40) Tarasevich M. R.; Sadkowski, A.; Yeager, E. *Comprehensive Treatise in Electrochemistry*; Plenum Press: New York, 1983; Chapter 6, pp 301−398.
(41) Pourbaix, M. *Atlas of electrochemical equilibria in aqueous solutions*; Pergamon Press: London, 1966; p 108.